

# Color Mismatches in Stereoscopic Video: Real-World Dataset and Deep Correction Method

Egor Chistov,\* Nikita Alutis,\* Maxim Velikanov,\* and Dmitriy Vatolin\*†

Lomonosov Moscow State University\*

MSU Institute for Artificial Intelligence†

{egor.chistov, nikita.alutis, maksim.velikanov, dmitriy}@graphics.cs.msu.ru

**Abstract**—We propose a real-world dataset of stereoscopic videos for color-mismatch correction. It includes real-world distortions achieved using a beam splitter. Our dataset is larger than any other for this task. We compared eight color-mismatch-correction methods on artificial and real-world datasets and showed that local methods are best suited to artificial distortions and that global methods are best suited to real-world distortions. Our efforts improved on the latest local neural-network method for color-mismatch correction in stereoscopic images, making it work faster and better on both artificial and real-world distortions.

**Index Terms**—color mismatches, stereoscopic video, beam splitter, real-world video dataset, color transfer

## I. INTRODUCTION

The left and right views of a stereoscopic image (stereopair) can have color mismatches for various reasons (e.g., illuminated camera filters, glare, and polarized light); Fig. 1 shows example. These mismatches can decrease the overall stereoscopic-video quality and may cause viewer discomfort and headaches [1].

Color-mismatch correction is the task of transferring color from one view of a stereopair to corresponding areas in another where the colors differ incorrectly. A sufficiently large dataset and sampling of color-mismatch types are crucial to comparing color-mismatch-correction methods. Previous datasets for this task either are too small or lack real-world mismatch examples. Therefore, we prepared a dataset using a beam splitter and three cameras that each captured a different view simultaneously: a distorted left view, a ground-truth left view, and a right view. In addition to containing real-world distortions, our dataset is thus far the largest for this task.

Despite the rapid development of deep learning, the latest neural-network method for correcting color mismatches [2] is still inferior to conventional alternatives. We improved it by making it run faster and better on both artificial and real-world distortions.

In this paper, we propose a real-world dataset of stereoscopic videos for color-mismatch correction as well as a method for color-mismatch correction of stereoscopic images. We also compared eight color-mismatch-correction methods on an artificial dataset and our real-world dataset. The code and datasets are at <https://github.com/egorchistov/color-transfer/>.

This study was supported by Russian Science Foundation under grant 22-21-00478, <https://rscf.ru/en/project/22-21-00478/>

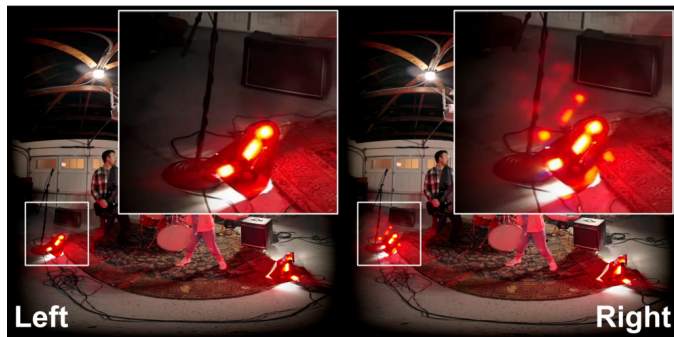


Fig. 1. Frame #1,200 from video “VR180 Cameras with Daydream,” taken by Google ([https://www.youtube.com/watch?v=TH\\_MMxInRsA/](https://www.youtube.com/watch?v=TH_MMxInRsA/)), contains color mismatches.

## II. RELATED WORK

This section provides an overview of stereoscopic datasets and methods for color-mismatch correction.

### A. Color-Mismatch-Correction Datasets

Few datasets are available for color-mismatch correction. They are either too small or lack real-world mismatches.

Niu et al. [3] employed 2D videos with parallel camera motion to extract pseudo-stereopairs without color mismatches; they gathered 18 source stereopairs. Using Photoshop CS6, they applied six different color operators—each with three severity levels—to one view of the stereopair.

Lavrushkin et al. [4] proposed gathering frames from stereoscopic movies produced only via 3D rendering to obtain undistorted stereopairs. They employed 1,000 FullHD frames. After adding color noise to one view of the stereopair, they smoothed the result by applying a domain transform filter.

Grogan et al. [5] chose image pairs captured by one camera under different illumination conditions, camera settings, and color touch-up styles. They aligned reference images to match the target images. Their dataset contains 15 image pairs with real-world mismatches.

The work of Croci et al. [2] used 1,035 stereopairs without color distortions from three different datasets. They applied six color operators—each with six severity levels—to one view of the stereopair using Photoshop 2021.

## B. Color-Mismatch-Correction Methods

The color-transfer problem is solvable globally or locally. Global methods [6, 7, 8] estimate a single color transformation for all pixels, and local methods [9, 4, 5, 2] do so for each pixel. Global methods do poorly on complex mismatches, and local methods produce inconsistent results in low-texture regions.

Reinhard et al. [6] proposed approximating an image as a three-dimensional Gaussian distributed signal. For each channel in the CIELAB color space, they used a linear model to transfer color from a reference image to the target image. They chose CIELAB because it is uncorrelated and allowed them to independently manipulate all three color channels.

Xiao et al. [7] computed a covariance matrix between color channels instead of treating them independently. The authors decomposed the covariance matrix using the SVD algorithm. They described the transformation as a scale, rotation, and shift of pixel clusters.

Pitié et al. [8] generalized all linear color-transfer approaches to the covariance-matrix fitting. They showed that the matrix decomposition this fitting implies can use the Cholesky decomposition, the square-root decomposition, or the solution to the Monge-Kantorovitch problem.

Pitié et al. [9] proposed using an iterative-distribution fitting to transfer color. This method iteratively projects target and reference images on random one-dimensional axes and performs a probability-density transfer along those axes. The authors reduced grain-noise artifacts by minimizing a special cost function.

Lavrushkin et al. [4] performed stereo matching with a modified cost function, making it better able to handle color mismatches between views. They applied a guided filter with a confidence-based variable-length kernel, using the left view as the target image and a warped right view as the guidance image.

Grogan et al. [5] proposed color transfer through estimation of the warping function that minimizes the divergence between two probability-density functions.

Croci et al. [2] employed a convolutional neural network for color-mismatch correction. First, the network extracts features from the input stereopair. It then feeds the extracted features into the parallax-attention mechanism [10], which performs stereo matching. Matched features pass through six residual blocks to yield the corrected stereoscopic view.

## C. Color Correction for Stitching Benchmarks

Some other datasets and methods can be found in Xu et al. [11] work. They evaluated the performance of nine color-correction methods for automatic multi-view image and video stitching on synthetic and real image pairs selected from different applications. Bellavia et al. [12] compared fifteen color correction algorithms for image stitching on three different existing real and artificial datasets.

## III. PROPOSED DATASET

We propose a new real-world dataset of stereoscopic videos for evaluating color-mismatch-correction methods. We collected it using a beam splitter and three cameras that simultaneously capture three views of a scene: a distorted left view, the ground-truth left view, and a right view. Compared to the simple camera-sliding-on-a-rail approach, the captured beam splitter distortions are closer to those seen in movies.

### A. Beam Splitter

A beam splitter is an optical device that divides light into a transmitted beam and a reflected beam. Because some light is lost owing to absorption by the reflective coating, this device introduces real-world mismatches between stereopair views. Similar mismatches can appear in stereoscopic movies filmed with a beam-splitter rig.

Our approach used a beam splitter to set a zero stereobase between the left camera and the left ground-truth camera, allowing us to create a distorted ground-truth data pair. A third camera captured the right view. Fig. 2 shows our setup.

We disabled optical stabilization and manually assigned all available camera settings, such as ISO, shutter speed, and color temperature. The cameras all had identical settings, so we obtained only beam-splitter distortions.

### B. Parallax Minimization

Filming the left distorted view and left ground-truth view without parallax is crucial to achieving precise ground-truth data. Parallax is a difference in the apparent position of an object when viewed along two lines of sight. Post-processing can precisely correct affine mismatches between views—namely scale, rotation angle, and translation—but it cannot correct parallax without using complex optical-flow, occlusion-estimation, and inpainting algorithms, which can reduce ground-truth-data quality.

We encountered a slight parallax due to inaccurate mounting of the cameras in our setup. To minimize it, we first visually aligned the lenses of the left distorted and left ground-truth cameras to obtain a visual zero stereobase. Then, using a

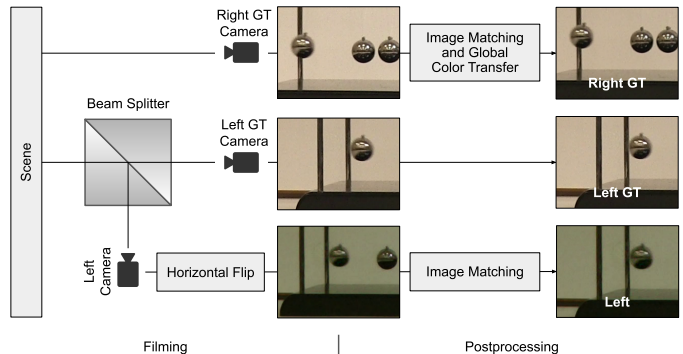


Fig. 2. Dataset filming and postprocessing pipeline. A beam splitter divides incoming light, which is then captured by the left camera and left ground-truth camera. The right camera captures the right ground-truth view. The final dataset frames have undergone spatial and temporal alignment.

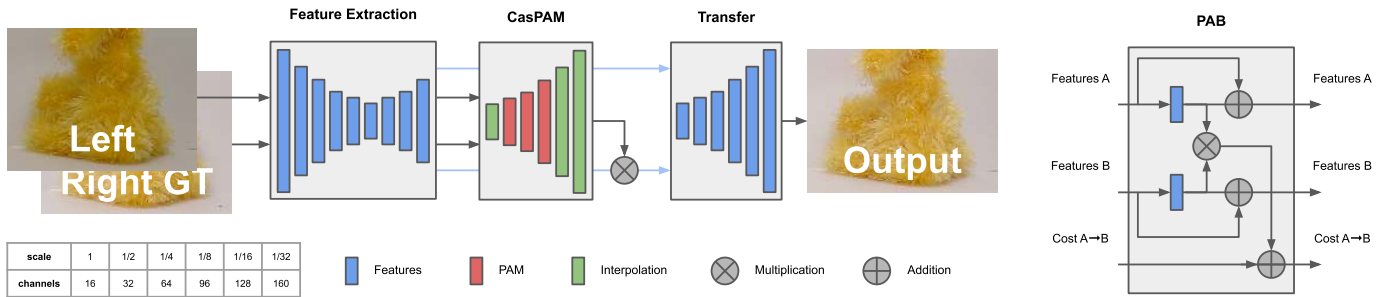


Fig. 3. Overview of proposed method for color-mismatch correction. Multiscale features extracted from the stereopair feed into the cascaded parallax-attention mechanism, which performs stereo matching. Matched features passed through the multiscale transfer module to yield the corrected left view.

photo from one camera and a video stream from another, we visualized the squared error between the views. This visualization allowed us to maximize the overlapping region by manually moving one camera. We achieved zero parallax through this method, but the manual alignment was time consuming.

### C. Postprocessing Pipeline

Our research employed the postprocessing pipeline in Fig. 2. Given the three videos from our cameras, we matched the horizontally flipped left distorted view to the left ground-truth view and rectified the stereopair using a homography transformation. To estimate the transformation parameters, we employed MAGSAC++ [13]. We selected SIFT [14] to match the left views, as well as the LoFTR [15] for rectification because LoFTR can better handle large parallax.

The technique of Pitié et al. [8] perfectly corrected the small loss in the transmitted beam. Without it, our approach would have been unable to obtain accurate ground-truth data. We performed temporal alignment using audio streams captured by the cameras: superimposing one stream on the other in the video editor allowed us to find the offset in frames.

### D. Scene Selection

Our research involved scenes in which an object rests on a table with a white background, 1.5 meters from the camera (Fig. 4). We filmed various objects including transparent glass, color patterns, and moving objects, choosing those that produced color mismatches. To ensure diversity, we filmed scenes under different lighting conditions, moving at different speeds, and we also used different cameras to ensure distortion variety. The lighting changed dynamically in one scene, and different scenes were shot with different set lighting.



Fig. 4. Example scenes from our dataset. It contains various objects that produce color mismatches.

We recorded most scenes in 4K resolution using three GoPro Hero 9 cameras. For the rest we recorded FullHD on two Legria HF G-10 cameras, one for the left ground-truth view and one for the right view, as well as a Panasonic HDC-SD800 for the left distorted view to add different camera distortions. The result was 24 scenes, each 50 frames long. We then cropped the region of interest to 960x720 pixels.

## IV. PROPOSED METHOD

Color-mismatch correction involves transferring color from one view of a stereopair to another in areas where colors incorrectly differ. Without limiting the task's generality, we propose a deep neural network that transfers color from the right view to the left view. The left corrected view should have a structure consistent with that of the left original view and colors consistent with those of the right view.

### A. Overview

We based our method on that of Croci et al. [2], borrowing ideas from Wang et al. [16]. Our contribution is an effective multiscale network structure that works faster and better on both artificial and real-world distortions. Our method consists of three main modules: feature extraction, cascaded parallax attention, and transfer. Fig. 3 shows the overall architecture.

### B. Feature-Extraction Module

The left and right views feed into the feature-extraction module to yield their color and structural features at scales from 1 to 1/32. This module consists of six encoder blocks and three decoder blocks. Each is a residual block with batch normalization and weighted skip connection. For downsampling we used strided convolutions, and for upsampling we used strided transposed convolutions. For each scale we kept the channel count unchanged, as Fig. 3 shows.

### C. Cascaded Parallax-Attention Module

Features from scales 1/16, 1/8, and 1/4 feed into the cascaded parallax-attention module (CasPAM) to obtain a multiscale warping-attention map. This module consists of three parallax-attention modules (PAM) and three interpolation layers. The interpolation layers allow us to obtain a warping-attention map at these scales whenever directly calculating an attention map is memory inefficient. Each PAM consist of four

TABLE I

COMPARISON OF EIGHT COLOR-MISMATCH-CORRECTION METHODS ON TWO DATASETS. THE BEST RESULT APPEARS IN **BOLD**; THE SECOND AND THIRD BEST ARE UNDERLINED. TIME MEASUREMENTS USED A PC BASED ON AN INTEL XEON SILVER 4216 PROCESSOR AND AN NVIDIA TITAN RTX GRAPHICS CARD WITH 24 GB OF MEMORY.

Method	Type	Time, ms↓	Artificial Dataset				Real-World Dataset			
			PSNR↑	SSIM↑	FSIMc↑	iCID↓	PSNR↑	SSIM↑	FSIMc↑	iCID↓
Reinhard et al. [6]	Global	246	31.1911	0.949414	0.982118	0.083559	<u>31.8822</u>	<b>0.870630</b>	<b>0.939015</b>	<u>0.123292</u>
Xiao et al. [7]	Global	168	30.2655	0.936797	0.977605	0.128691	28.2195	0.809752	0.913462	0.229490
Pitié et al. [8]	Global	<u>167</u>	32.2269	<u>0.963368</u>	<b>0.987697</b>	<u>0.057986</u>	<b>32.0452</b>	<u>0.869496</u>	<u>0.937853</u>	<b>0.122708</b>
Pitié et al. [9]	Local	1220	30.6422	0.960669	0.977523	0.084648	<u>31.9461</u>	0.865658	0.927836	<u>0.125855</u>
Lavrushkin et al. [4]	Local	<u>118</u>	<b>34.8593</b>	<b>0.972175</b>	<u>0.987143</u>	<u>0.050135</u>	<u>30.3340</u>	0.865228	0.933478	<u>0.127936</u>
Grogan et al. [5]	Local	1525	<u>34.2358</u>	0.969720	<u>0.984778</u>	<b>0.044421</b>	30.8256	0.868088	0.936303	0.133320
Croci et al. [2]	NN-based	285	28.8919	0.961064	0.978339	0.092929	27.3275	0.858226	0.921545	0.150149
Ours	NN-based	<b>109</b>	<u>32.5703</u>	0.961326	0.983307	0.074452	28.6305	0.861331	0.926881	0.161298

parallax-attention blocks (PAB) [10]. Every block updates the input features and converts them to a query and a key. After multiplying the query by the key, we added the result to the matching attention map. Our last step was to apply lower triangular softmax to this map and multiply the result by the right view’s features to obtain warped right view’s features.

#### D. Transfer Module

The transfer module concatenates the valid mask, the left-view, and warped-right-view features at scales from  $1/32$  to 1. A valid mask indicates pixels that match in another view. Then, for each scale we added upsampled features from the previous scale to features from the current scale and passed the result through residual block without batch normalization. The residual block’s output for scale 1 is the corrected left view.

#### E. Loss Function

We trained our network using the  $\mathcal{L}_1$ ,  $\mathcal{L}_2$ , and  $\mathcal{L}_{SSIM}$  loss functions applied to the corrected left view and ground-truth left view. We trained our cascaded parallax-attention module without ground-truth attention maps using the photometric  $\mathcal{L}_{PH}$ , smoothness  $\mathcal{L}_{SM}$ , and cycle-consistency  $\mathcal{L}_{CC}$  loss functions, as Wang et al. [10] described.

### V. EXPERIMENTS

To compare our method with seven others we chose two datasets and four image quality assessment methods.

#### A. Artificial Dataset

The first dataset contained undistorted stereopairs from the same sources as Croci et al. [2] proposed. To exclude stereopairs with color mismatches, we analyzed them automatically by measuring the average absolute difference between two matched views and discarding stereopairs with large differences. The final result was 1,035 undistorted stereopairs.

Instead of employing Photoshop 2021 as Croci did, we applied color augmentations to the left view of the stereopair. We split the dataset into three parts: training (835 stereopairs), validation (100 stereopairs), and test (100 stereopairs).

#### B. Real-World Dataset

The second dataset, described in Section III, contains the distortions we encountered while shooting stereoscopic videos using a beam splitter. We again divided the dataset into three parts: training (900 stereopairs), validation (150 stereopairs), and test (150 stereopairs).

#### C. Training Procedure

We trained our network with the Adam optimizer over 100 epochs on the artificial dataset using random patches of size  $512 \times 256$ . The learning rate was 0.0001 and the batch size was 16. The network converged in 1.5 hours on a PC with an Intel Xeon Silver 4216 processor and Nvidia Titan RTX GPU with 24 GB of memory. Next, we fine-tuned all the neural-network-based methods on the real-world dataset over another 50 epochs at a learning rate of 0.0001. Our study found that in order to achieve higher scores on real-world distortions, one needs to fine-tune using artificial distortions with real-world ground truth stereopairs. When fine-tuning degraded the quality of the model, we used the untuned model.

#### D. Quality Metrics

Our evaluation used four full-reference image quality assessment (IQA) methods: peak signal to noise ratio (PSNR), structural similarity (SSIM) index, feature similarity for color images (FSIMc) index, and improved color-image-difference (iCID) metric. To incorporate color information, since PSNR and SSIM work on gray images, we apply them to individual

TABLE II

ABLATION STUDY OF PROPOSED COLOR-MISMATCH-CORRECTION METHOD ON THE ARTIFICIAL DATASET’S VALIDATION PART. THE UPPER PORTION OF THE TABLE SHOWS EXPERIMENTS WITH LOSS FUNCTIONS; THE LOWER PORTION SHOWS EXPERIMENTS WITH THE ARCHITECTURE.

Description	PSNR↑	SSIM↑
With perceptual loss $\mathcal{L}_{perc}$ based on VGG	30.439	0.9636
$\mathcal{L}_{huber}$ instead of $\mathcal{L}_1$ , $\mathcal{L}_2$ , and $\mathcal{L}_{SSIM}$	31.322	0.9448
Without $\mathcal{L}_{PH}$ , $\mathcal{L}_{SM}$ , and $\mathcal{L}_{CC}$ losses	32.621	0.9661
Without weighted shortcut in residual blocks	31.711	0.9623
Billinear upsample instead of transposed conv	31.878	0.9671
Final	32.747	0.9680

channels of the RGB color space and average the channel scores for the final score. Detailed IQA methods quality analysis can be found in Niu et al. [3] work. Also, we measured the time each method took to process one 512x512 frame. We repeated these measurements three times and in each case reported the shortest time in milliseconds.

### E. Ablation Study

We conducted an ablation study (Table II) on the validation part of the artificial dataset. Our conclusion is that the combination of the  $\mathcal{L}_1$ ,  $\mathcal{L}_2$ ,  $\mathcal{L}_{SSIM}$ , and  $\mathcal{L}_{PH}$ ,  $\mathcal{L}_{SM}$ ,  $\mathcal{L}_{CC}$  loss functions is optimal and that all architectural components contribute to our network quality.

Our study found that neural networks generalize much better to the unseen distortion type by using the valid mask. We also noticed that the batch-normalization layers in the transfer module yielded strong visible artifacts, so we disabled them in this module.

### F. Comparison Study

We compared the proposed method (see Table I and Fig. 5) with three global methods [6, 7, 8], one local method [9], two correspondence-based local methods [4, 5], and one neural-network-based local method [2].

As Table I shows, local methods perform better on artificial distortions and global methods perform better on real-world distortions. Local methods do worse on the real-world dataset because of inconsistent results in low-texture regions; global methods do worse on the artificial dataset because the artificial distortions are nonlinear.

Our neural-network-based method is ranked higher than Croci's [2] by all quality metrics on the artificial dataset and by three out of four quality metrics on the real-world dataset, and also our method is 2.6 times faster. However, it is not enough to outperform the conventional methods, which warranting further investigation.

## VI. CONCLUSION

Few datasets are available for evaluating color-mismatch-correction methods. Most of them are either too small or lack real-world mismatches. We created a new large-scale dataset of real-world stereoscopic videos to perform this task. We also showed that global and local methods produce different results on artificial and real-world datasets, and that neural-network-based methods fall short of conventional methods. We improved the latest neural-network method for correcting color mismatches and hope our contribution will enable development of methods that perform better on both artificial and real-world datasets.

## REFERENCES

[1] A. Antsiferova and D. Vatolin, "The influence of 3d video artifacts on discomfort of 302 viewers," in *2017 International Conference on 3D Immersion (IC3D)*. IEEE, 2017, pp. 1–8.

[2] S. Croci, C. Ozcinar, E. Zerman, R. Dudek, S. Knorr, and A. Smolic, "Deep color mismatch correction in stereoscopic 3d images," in *2021 IEEE International Conference on Image Processing (ICIP)*, 2021, pp. 1749–1753.

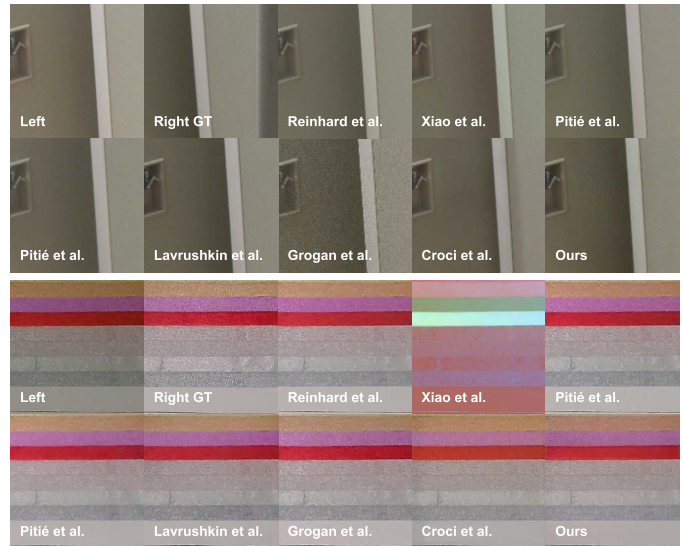


Fig. 5. Examples of color-mismatch correction. The first stereopair is from the artificial dataset; the second is from the real-world dataset.

[3] Y. Niu, H. Zhang, W. Guo, and R. Ji, "Image quality assessment for color correction based on color contrast similarity and color value difference," *IEEE Transactions on Circuits and Systems for Video Technology*, vol. 28, no. 4, pp. 849–862, 2016.

[4] S. Lavrushkin, V. Lyudvichenko, and D. Vatolin, "Local method of color-difference correction between stereoscopic-video views," in *2018 - 3DTV-Conference: The True Vision - Capture, Transmission and Display of 3D Video (3DTV-CON)*, 2018, pp. 1–4.

[5] M. Grogan and R. Dahyot, "L2 divergence for robust colour transfer," *Computer Vision and Image Understanding*, vol. 181, pp. 39–49, 2019.

[6] E. Reinhard, M. Ashikhmin, B. Gooch, and P. Shirley, "Color transfer between images," *IEEE Computer Graphics and Applications*, vol. 21, pp. 34–41, 2001.

[7] X. Xiao and L. Ma, "Color transfer in correlated color space," in *Proceedings of the 2006 ACM international conference on Virtual reality continuum and its applications*, 2006, pp. 305–309.

[8] F. Pitié and A. Kokaram, "The linear monge-kantorovitch linear colour mapping for example-based colour transfer," in *IET 4th European Conference on Visual Media Production*. IEE, 2007, pp. 1–9.

[9] F. Pitié, A. Kokaram, and R. Dahyot, "Automated colour grading using colour distribution transfer," *Computer Vision and Image Understanding*, vol. 107, no. 1–2, pp. 123–137, 2007.

[10] L. Wang, Y. Guo, Y. Wang, Z. Liang, Z. Lin, J. Yang, and W. An, "Parallax attention for unsupervised stereo correspondence learning," *IEEE Transactions on Pattern Analysis and Machine Intelligence*, vol. 44, no. 4, pp. 2108–2125, 2020.

[11] W. Xu and J. Mulligan, "Performance evaluation of color correction approaches for automatic multi-view image and video stitching," in *2010 IEEE computer society conference on computer vision and pattern recognition*. IEEE, 2010, pp. 263–270.

[12] F. Bellavia and C. Colombo, "Dissecting and reassembling color correction algorithms for image stitching," *IEEE Transactions on Image Processing*, vol. 27, no. 2, pp. 735–748, 2017.

[13] D. Barath, J. Noskova, M. Ivashechkin, and J. Matas, "Magsac++, a fast, reliable and accurate robust estimator," in *Proceedings of the IEEE/CVF conference on computer vision and pattern recognition*, 2020, pp. 1304–1312.

[14] D. Lowe, "Distinctive image features from scale-invariant keypoints," *International journal of computer vision*, vol. 60, pp. 91–110, 2004.

[15] J. Sun, Z. Shen, Y. Wang, H. Bao, and X. Zhou, "Loft: Detector-free local feature matching with transformers," in *Proceedings of the IEEE/CVF conference on computer vision and pattern recognition*, 2021, pp. 8922–8931.

[16] Y. Wang, J. Peng, Y. Zhang, S. Liu, X. Sun, and Z. Xiong, "Asymmetric stereo color transfer," in *2021 IEEE International Conference on Multimedia and Expo (ICME)*. IEEE, 2021, pp. 1–6.